*J. Indian Inst. Sci.*, Mar.–Apr. 1988, 68, 109–128


# Membrane analysis and load-deflection behaviour of isotropic simply supported reinforced concrete circular slabs

PRAKASH DESAYI AND K. U. MUTHU*
Department of Civil Engineering, Indian Institute of Science, Bangalore 560 012, India.

Received on May 14, 1986; Revised on August 20, 1987.

**Abstract**

Load-deflection relation of isotropic simply supported reinforced concrete circular slabs subjected to distributed load has been determined taking into account the effect of membrane action for loads greater than the yield-line load. The analysis includes the effect of deflections occurring up to yield-line load. Results are compared with those of tests conducted in the laboratory.

**Key words:** Concrete (reinforced), deflection, loads, membrane action, reinforcement (isotropic), slabs (circular), yield-line load.

## 1. Introduction

The yield-line theory proposed by Johansen[1] has been widely used for the design of irregular type of slabs having different types of boundary conditions and loadings. This theory is finding acceptance due to the fact that the ultimate loads as determined in tests[2] are much higher than those predicted by yield-line theory. This difference between yield-line load and experimental load is due to the development of membrane stresses at large deflections in simply supported slabs at midspan. In simply supported slabs, the central regions tend to move inwards but are restrained from doing so by adjacent outer regions. This creates a central area of tensile membrane stresses within the slab together with the surrounding ring of compression. This effect enhances the load-carrying capacity of the slab. Park[3], Taylor *et al*[4], Hayes[5], Kemp[6], Sawczuck and Winnicki[7], Morley[8] and Desayi and Kulkarni[9] proposed methods of analysis for rectangular simply supported reinforced concrete slabs including membrane action. Prabhakara[10] extended the work of Desayi and Kulkarni to simply supported skew slabs. The above investigations were concerned with rectangular and skew slabs.

*Present address: Department of Civil Engineering, M.S. Ramaiah Institute of Technology, Bangalore 560 054, India.

Membrane action in isotropic circular slabs was analysed by Wood[11] using basic equations of large deflection plate theory. Due to the basic assumption that the material is rigid plastic, the resulting load-deflection curve starts from Johansen's load and so zero load does not correspond to zero deflection. However, Wood's analysis is useful to estimate the ultimate strength of slab if a suitable value of deflection at ultimate load is assumed. Desayi and Kulkarni[12] extended Wood's approach to orthotropic restrained circular slabs. While the above investigations were based on deformation theory, some investigators have applied flow theory to circular slabs. Janas[13], Morley[8], Calladine[14], have applied flow theory to circular slabs. Al-Hassani[15] used deformation theory for the ascending part of the load-deflection curve and flow theory for the descending portion of the curve. Braestrup and Morley[16] proposed a modified rigid plastic theory for circular slabs with ring beams. They assumed that membrane action starts an initial elastic deflection. This deflection was assumed empirically as 0.03 times the thickness of slab. From their load-deflection plots, it is observed that the empirical elastic deflection corresponds to that at the Johansen's load of simply supported circular slabs. Chattopadhayay[17] gave some steps to obtain the initial value of deflection according to the theory presented in their paper.

The above investigations on circular slabs were concerned with rigid plastic approach and they do not completely predict the load-deflection behaviour from zero load to failure, as seen in an experiment. Hence, a study was undertaken to develop methods for the determination of complete load-deflection behaviour of simply supported, isotropic circular slabs and the results of the same are briefly presented here.

## 2. Proposed method

The method has been developed in three stages. Figure 1 shows the typical load-deflection plot in which AB, BC and CD correspond to three stages. In the first stage (AB), classical theory of plates is used for computing deflections up to cracking load. In the second stage (BC), an effective moment of inertia is used which reflects the reduction in flexural rigidity of the slab beyond cracking. Third stage (CD) corresponds to the prediction of the behaviour of the slab beyond Johansen's load incorporating the effect of membrane action.

### 2.1. *Stage 1: Load-deflection behaviour up to cracking load*

In fig. 1, AB represents the elastic behaviour and the central deflection $\delta$ of the slab up to point B is estimated using classical plate theory[18]. Thus

$$\delta = \frac{\beta_1 \, q \, R^4}{E_c \, I_g} \tag{1}$$

where $\beta_1 = \beta/(1-\mu^2)$

$\beta = (5+\mu)/64(1+\mu)$

and $\mu$ = Poisson's ratio taken equal to 0.2 for concrete

$q$ = intensity of load

$R$ = radius of circular plate

$E_c$ = modulus of elasticity of concrete

$I_g$ = gross momentum of inertia of the section.

The value of $E_c$ is taken as $4729\sqrt{f'_c}$ $N/mm^2$ where $f'_c$ is in $N/mm^2$ ($57000\sqrt{f'_c}$ psi where $f'_c$ is in psi)[19].

At $B$ in fig 1, $\delta = \delta_{cr}$ and from equation (1)

$$\delta_{cr} = \frac{\beta_1 . q_{cr} R^4}{E_c I_g} \tag{2}$$

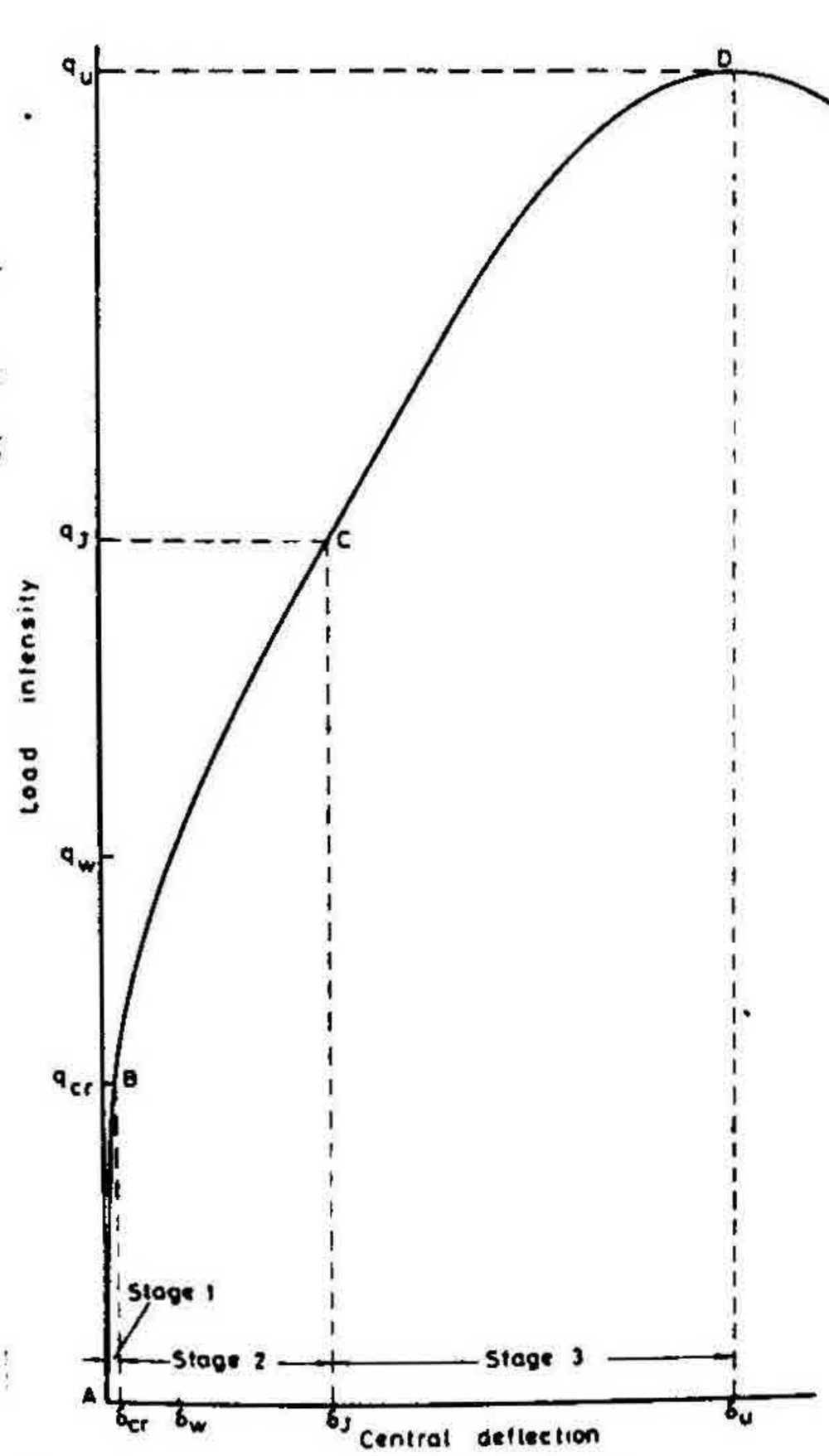


FIG. 1. Idealised load-deflection plot.

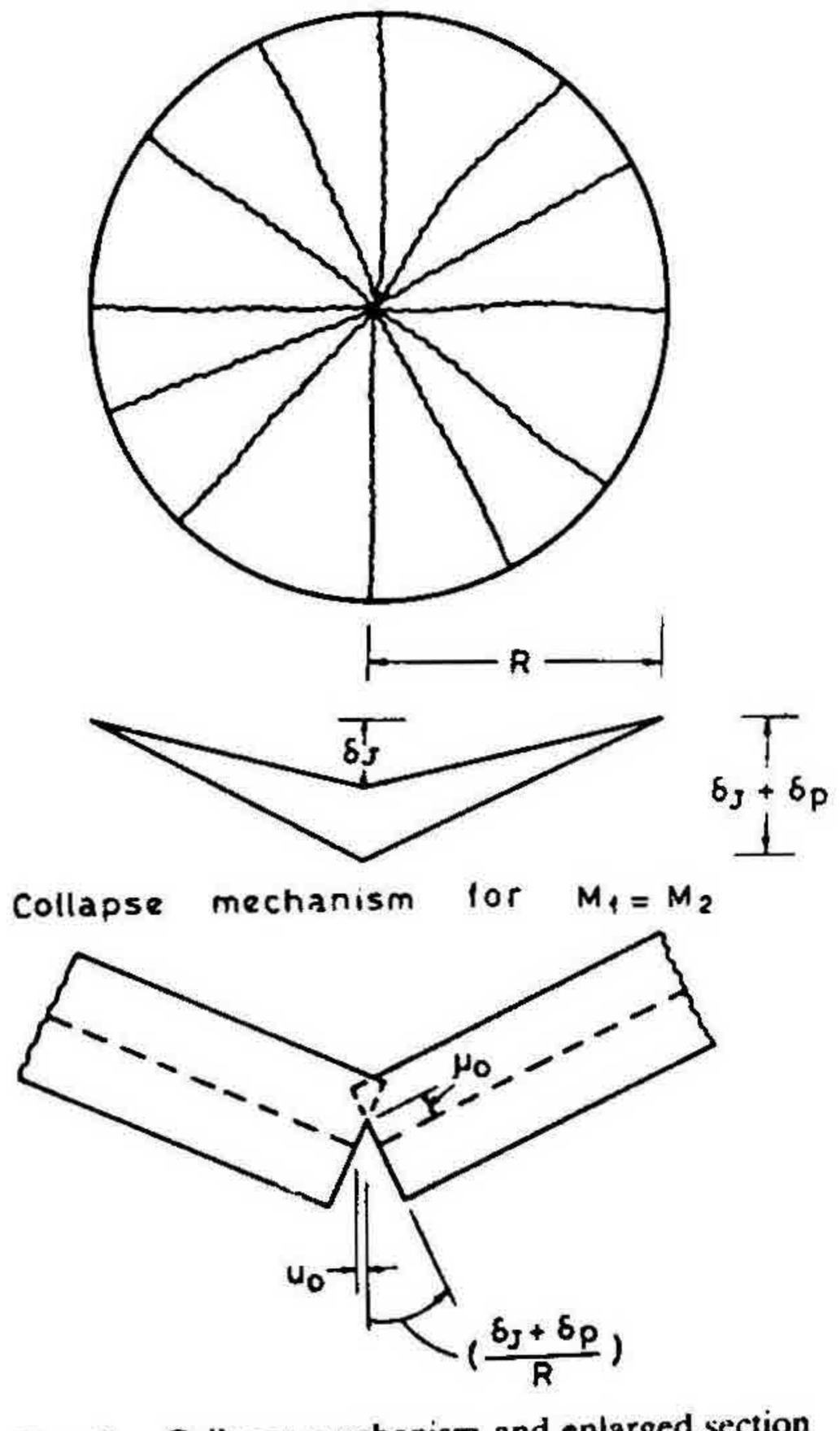


FIG. 2. Collapse mechanism and enlarged section at the centre of the slab.

in which

$q_{cr}$ = intensity of cracking load

which is determined by equating the slab moment at the centre, *viz.*,

$$m_\theta = m_r = \frac{(3+\mu)qR^2}{16} \tag{3}$$

to the cracking moment, *viz.*,

$$m_{cr} = f_r I_g / y_t. \tag{4}$$

The value of $f_r$ in equation (4) is taken as $0.6225\sqrt{f_c'}$ $N/mm^2$ where $f_c'$ is in $N/mm^2$ ($7.5\sqrt{f_c'}$ psi where $f_c'$ is in psi)[20].

### 2.2. *Stage 2: Load-deflection behaviour beyond cracking load and up to Johansen's load*

As a consequence of cracking of concrete the flexural rigidity decreases as the load increases beyond cracking load. Hence equation (1) is modified to

$$\delta = \frac{\beta_1 q R^4}{k_s E_c I_{\text{eff}}} \tag{5}$$

where $k_s$ is a constant and

$$I_{\text{eff}} = \left(\frac{q_{cr}}{q}\right)^\gamma I_g + \left[1 - \left(\frac{q_{cr}}{q}\right)^\gamma\right] I_{cr} \tag{6}$$

in which $\gamma$ is a constant, $I_{cr}$ is cracked moment of inertia of the section and $q > q_{cr}$.

Two coefficients $k_s$ and $\gamma$ were introduced to improve on the prediction of deflections. Hence at an intensity of load $q$ which is in the range $q_{cr} < q < q_j$, the deflection $\delta$ can be determined using equations (5) and (6). In order to use these equations $k_s$ and $\gamma$ must be evaluated. This has been done using the results of an experimental programme, the details of which have been reported elsewhere[19].

### 2.3. *Stage 3: Load-deflection behaviour beyond Johansen's load*

In this stage the load-deflection behaviour beyond Johansen's load is determined by a procedure which incorporates membrane action. The procedure has been developed for both isotropic and polar orthotropic circular slabs. Wood's solution[11] for isotropic circular slabs has been modified by including the effect of deflections prior to Johansen's load on the depth of neutral axis, membrane forces and their effect on load-carrying capacity. The solution derived for isotropic circular slabs only is presented in this paper.

### 2.4. *Strain rates imposed by mechanism*

Figure 2 shows the yield-line pattern of a simply supported circular slab with radius $R$. The mechanism beyond Johansen's load can be described with the assumption that the membrane forces are introduced after yield-line mechanism forms at Johansen's load as

$$W = (\delta_j + \delta_p)\,(1 - r/R) \tag{7}$$

where $W$ is the deflection and $\delta_j$, $\delta_p$ are deflections at the centre at Johansen's load and incremental deflection beyond Johansen's load. Hence

$$\frac{dW}{dr} = -\frac{(\delta_j + \delta_p)}{R}\,. \tag{8}$$

The radial strain $\varepsilon_r$ can be obtained from large deflection plate theory as[11]

$$\varepsilon_r = \frac{du}{dr} + \frac{1}{2}\left(\frac{dw}{dr}\right)^2 \tag{9}$$

where $u$ is the radial displacement which can be determined as follows. The value of $\varepsilon_r$ in equation (9) is zero as the yielding is due to circumferential moments only. Hence equation (9) becomes

$$\frac{du}{dr} + \frac{1}{2}\left(\frac{dw}{dr}\right)^2 = 0. \tag{10}$$

Substituting for $(dw/dr)$ from equation (8) in equation (10) and integrating,

$$u = -\frac{1}{2}\,\frac{(\delta_j + \delta_p)^2 r}{R^2} + u_0 \tag{11}$$

where $u_0$ is the finite stretch at half-depth imposed at the centre. Thus $u$ is known. From this, the circumferential strain $\varepsilon_\theta$ can be determined as,

$$\varepsilon_\theta = \frac{u}{r} = -\frac{1}{2}\,\frac{(\delta_j + \delta_p)^2}{R^2} + \frac{u_0}{r}\,. \tag{12}$$

If $\mu_0$ is the height of neutral axis above mid-depth, equation (12) can be rewritten as follows. From fig. 2, the value of $u_0$ is related to $\mu_0$ as

$$u_0 = \frac{\mu_0(\delta_p + \delta_j)}{Rr}\,. \tag{12a}$$

Substituting this value of $\mu_0$ in equation (12), we get

$$\varepsilon_\theta = \frac{\mu_0(\delta_p + \delta_j)}{Rr} - \frac{1}{2}\,\frac{(\delta_j + \delta_p)^2}{R^2 r}\,. \tag{13}$$

The circumferential curvature $K_\theta$ can be obtained from equation (8) as

$$K_\theta = -\frac{1}{r}\,\frac{dW}{dr} = \frac{(\delta_j + \delta_p)}{Rr}\,. \tag{14}$$

Knowing $\varepsilon_\theta$ from equation (13) and $K_\theta$ from equation (14), the height of neutral axis above mid-depth in circumferential direction, $\mu_\theta$ can be obtained as

$$\mu_\theta = \frac{\varepsilon_\theta}{K_\theta} = \mu_0 - \frac{(\delta_j + \delta_p)r}{2R}\,. \tag{15}$$

The height of neutral axis can also be calculated from yield criterion which is presented in the next section.

*2.5 Yield criterion*

Wood[5] proposed the yield criterion for isotropic circular slabs as

$$\frac{M}{M_0} = 1 + \alpha\,\frac{P}{T_0} - \beta\,\frac{P^2}{T_0^2} \tag{16}$$

and hence the yield function

$$f = 1 + \alpha\,\frac{P}{T_0} - \beta\,\frac{P^2}{T_0^2} - \frac{M}{M_0} \tag{17}$$

where $M$ and $P$ are the plastic moment capacity of the section about the central line and the compressive force on unit width respectively. Also $M_0$ and $T_0$ are the plastic moment capacity of the section with zero membrane stress and uniaxial tension respectively[5] *i.e.*

$$M_0 = A_s f_y \mathrm{d}_1 \left(1 - \frac{3}{4}\,\frac{A_s}{bd_1}\,\frac{f_y}{f_c}\right) \tag{17a}$$

and

$$T_0 = A_s f_y\,. \tag{17b}$$

Substituting the value of $T_0$ from equation (17b) in equation (17a) we get

$$M_0 = \frac{T_0 \mathrm{d}}{k} \tag{17c}$$

where

$$k = \frac{\mathrm{d}/\mathrm{d}_1}{1 - \frac{3}{4}\frac{A_s}{bd_1}\frac{f_y}{f_c}} \,. \tag{17d}$$

Considering the yield criterion in circumferential direction only, equation (17) becomes

$$f_\theta = 1 + \alpha \frac{P_\theta}{T_0} - \beta \frac{P_\theta^2}{T_0^2} - \frac{M_\theta}{M_0} \tag{18}$$

where $M_\theta$ and $P_\theta$ are plastic moment capacity along the centre line and the overall compressive force in circumferential direction only. The constants $\alpha$ and $\beta$ in equations (16–18) are defined as follows[5]

$$\alpha = \frac{\frac{1}{2}\frac{\mathrm{d}}{\mathrm{d}_1} - \frac{3}{2}t}{1 - \frac{3}{4}t} \tag{19}$$

$$\beta = \frac{\frac{3}{4}t}{1 - \frac{3}{4}t} \tag{20}$$

and $$t = \frac{A_s f_y}{\mathrm{d}_1 f_c} \,. \tag{21}$$

Hence, from the yield function in circumferential direction, *viz.*, equation (18), the height of neutral axis in circumferential direction is determined as.

$$\mu_\theta = -\frac{\partial f_\theta / \partial P_\theta}{\partial f_\theta / \partial M_\theta} = M_0 \left[\frac{\alpha}{T_0} - \frac{2\beta P_\theta}{T_0^2}\right] . \tag{22}$$

Equating (15) and (22), we obtain

$$\frac{P_\theta}{T_0} = A + Br \tag{23}$$

where $$A = \frac{\alpha}{2\beta} - \frac{\mu_0 T_0}{2\beta M_0} \tag{24}$$

and $$B = \frac{(\delta_f + \delta_p) T_0}{4\beta M_0 R} . \tag{25}$$

Knowing $P_\theta$ from equation (23), the value of $M_\theta$ can be obtained from the yield criterion equation (16) as

$$\frac{M_\theta}{M_0} = (1 + \alpha A - \beta A^2) + (\alpha B - 2\beta A B) r - \beta B^2 r^2$$

$$= A_1 + B_1 r + C_1 r^2 \tag{26}$$

where $$A_1 = 1 + \alpha A - \beta A^2 \tag{27}$$

$$B_1 = \alpha B - 2\beta A B \tag{28}$$

$$C_1 = -\beta B^2. \tag{29}$$

*2.6. Evaluation of radial force and moment*

The value of the radial force $T_r$ and the radial moment $M_r$ are obtained from the equilibrium equation. In the plane of the slab the equilibrium equation is[11]

$$\frac{\mathrm{d}}{\mathrm{d}r}\left(r \frac{T_r}{T_0}\right) = \frac{T_\theta}{T_0} = -\frac{P_\theta}{T_0} \tag{30}$$

from which

$$\frac{T_r}{T_0} = -A - \frac{Br}{2} + \frac{C}{r} . \tag{31}$$

The value of $C$ in equation (31) is zero and also $T_r = 0$ at $r = R$. Using these conditions in equation (31), the value of $A$ is obtained as

$$A = -\frac{BR}{2} . \tag{32}$$

Hence equation (31) reduces to

$$\frac{T_r}{T_0} = -\frac{BR}{2} - \frac{Br}{2}. \tag{33}$$

The value of $M_r$ is evaluated using the equilibrium equation for moments which includes the membrane forces. The equilibrium equation is[11]

$$\frac{\mathrm{d}}{\mathrm{d}r}(rM_r) - M_\theta + rT_r \frac{\mathrm{d}w}{dr} = -\frac{qr^2}{2}. \tag{34}$$

Substituting for $M_\theta$ and $T_r$ from equations (26) and (33) in equation (34) and integrating we obtain the value of $M_r$ as,

$$\frac{M_r}{M_0} = \frac{r}{2}\left[B_1 - \frac{(\delta_j+\delta_p)T_0 A}{RM_0}\right] + \frac{r^2}{3}\left[C_1 - \frac{(\delta_j+\delta_p)BT_0}{2RM_0}\right] + \frac{a}{r} + b - \frac{qr^2}{6M_0}. \tag{35}$$

In equation (35), the value of $a$ is zero as the value of $M_r$ is finite at the centre. The values of $b$ and $q$ are obtained using two conditions which are as follows. At the centre of the slab $M_r = M_\theta$ and hence from equation (26),

$$\left(\frac{M_r}{M_0}\right)_{r=0} = \left(\frac{M_\theta}{M_0}\right)_{r=0} = A_1. \tag{36}$$

At the edge of the slab the value of the radial moment is zero. Hence

$$(M_r)_{r=R} = 0. \tag{37}$$

Substituting equations (36) and (37) in equation (35)

$$\frac{qR^2}{6M_0} = 1 + \alpha A - \beta A^2 + \frac{R}{2}\left[\alpha B - 2\beta AB - \frac{AT_0}{RM_0}(\delta_j+\delta_p)\right] - \frac{R^2}{3}\left[\beta B^2 + \frac{BT_0}{2rM_0}(\delta_j+\delta_p)\right]. \tag{38}$$

Substituting the values of $A$ from equation (24) and using the relation between $A$ and $B$ from equation (32) in equation (38), we get

$$\frac{qR^2}{6M_0} = 1 - \frac{\alpha(\delta_j+\delta_p)T_0}{8\beta M_0} - \frac{\beta B^2 R^2}{4} + \frac{\alpha(\delta_j+\delta_p)T_0}{8\beta M_0} + \frac{\beta B^2 R^2}{2}$$

$$+ \frac{T_0^2(\delta_j+\delta_p)^2}{6\beta M_0^2} - \frac{T_0^2(\delta_j+\delta_p)^2}{16\beta M_0^2} = 1 + \frac{\beta B^2 R^2}{4} . \quad (39)$$

Substituting the value of $B$ from equation (25) and using equation (17c) in equation (39) we get

$$\frac{qR^2}{6M_0} = 1.0 + (k^2/64\beta)\left(\frac{\delta_j+\delta_p}{\mathrm{d}}\right)^2 . \quad (40)$$

The above equation reduces to

$$\frac{Q_m}{Q_j} = 1.0 + \frac{k^2}{64\beta}\left(\frac{\delta_j+\delta_p}{\mathrm{d}}\right)^2 \quad (41)$$

where $Q_m$ is the enhanced load due to membrane action *i.e.*

$$Q_m = \pi R^2 q \quad (42a)$$

and yield-line load

$$Q_j = 6\pi M_0 . \quad (42b)$$

This total load $Q_m$ increases until a new state of tensile membrane develops at the centre. When $\mu_0 = \mathrm{d}/2$ the plastic membrane develops. The shape of the plastic membrane is obtained from the equilibrium equations as follows.

### 2.7. *Effect of plastic membrane at centre*

The equilibrium equation for the radial moments is[11]

$$\frac{\mathrm{d}}{\mathrm{d}r}(rM_r) - M_\theta - r\,V_r = 0 \quad (43)$$

and the equilibrium equation for the vertical forces is

$$\frac{\mathrm{d}}{\mathrm{d}r}(r\,V_r) + \frac{\mathrm{d}}{\mathrm{d}r}\left(r\,T_r\frac{\mathrm{d}W}{\mathrm{d}r}\right) = -qr. \quad (44)$$

Now a state of all round tension exists and hence it is assumed that,

$$M_r = M_\theta = M_{\min} = M_0(1-\alpha-\beta) \tag{45}$$

$$T_r = T_\theta = T_0. \tag{46}$$

Substituting the values of $M_r$, $M_\theta$ from equation (45) in equation (43) we get

$V_r = 0$ *i.e.* there is no shear.

Substituting the value of $V_r = 0$ and $T_r = T_0$ from equation (46) in equation (44), we obtain

$$\frac{\mathrm{d}}{\mathrm{d}r}\left(r\,T_0\,\frac{\mathrm{d}W}{\mathrm{d}r}\right) = -qr. \tag{47}$$

This leads to

$$\frac{\mathrm{d}W}{dr} = -\frac{qr}{2T_0} \tag{48}$$

or, $$W = (\delta_p + \delta_j) - \frac{qr^2}{4T_0}\cdot \tag{49}$$

From equation (48), the curvatures $K_r$ and $K_\theta$ are obtained as

$$K_r = -\frac{\mathrm{d}^2 W}{\mathrm{d}r^2} = \frac{q}{2T_0}\cdot \tag{50}$$

$$K_\theta = -\frac{1}{r}\,\frac{\mathrm{d}W}{\mathrm{d}r} = \frac{q}{2T_0}\cdot \tag{51}$$

From equations (50) and (51), it is known that the plastic membrane is of spherical shape and at this stage the slab would have cracked right through. Due to this the extension rates could be different, but are the same at the centre. Hence Wood[11] assumed that they are identical everywhere and so

$$\frac{u}{r} = \frac{\mathrm{d}u}{\mathrm{d}r} + \frac{1}{2}\left(\frac{\mathrm{d}W}{\mathrm{d}r}\right)^2 \tag{52}$$

and this leads to

$$u = \frac{-q^2 r^3}{16\,T_0^2\cdot} + Cr \tag{53}$$

where $C$ is an arbitrary constant. The membrane will change to an outer cone at radius $\rho$ and hence the displacement at the junction is

$$u_\rho = \frac{-q^2\rho^3}{16T_0^2} + C\rho. \tag{54}$$

Also the value of deflection at radius $\rho$ can be determined for the outer cone as follows. For the outer cone,

$$\frac{dW}{dr} = \frac{-W_\rho}{R-\rho}. \tag{55}$$

Since the yielding is due to circumferential moments only for the outer cone $\varepsilon_r = 0$ and hence using equations (10) and (55) the displacement $u$ is obtained as

$$P_\theta = A_2 + B_2 r \tag{56}$$

where

$$A_2 = T_0\frac{\alpha}{2\beta} - \frac{T_0^2}{2\beta M_0}\left[\frac{W_\rho\rho}{2(R-\rho)} + \frac{u_\rho(R-\rho)}{W_\rho}\right] \tag{57}$$

and

$$B_2 = \frac{T_0^2}{2\beta M_0}\left[\frac{W_\rho}{2(R-\rho)}\right]. \tag{58}$$

Hence at $r = \rho$, if $P_\theta = -T_0$ then

$$A_2 = -T_0 - B_2\rho. \tag{59}$$

Substituting equation (59) in equation (56) the value of $P_\theta$ is

$$P_\theta = -T_0 + B_2 R\left(\frac{r}{R} - \frac{\rho}{R}\right). \tag{60}$$

Substituting equation (60) in the equilibrium equation of forces in the plane of the slab *i.e.* equation (30) we get

$$T_r = -A_2 - \frac{B_2 r}{2} + \frac{C_2}{r} \tag{61}$$

and since $T_r = 0$ when $r = R$ and $T_r = T_0$ when $r = \rho$,

$$T_r = -A_2 - \frac{B_2 R}{2}\,\frac{r}{R} + \left(A_2 + \frac{B_2 R}{2}\right)\frac{R}{r} \tag{62}$$

and also $$B_2 R = \frac{2T_0}{(1-\rho/R)^2}\,. \tag{63}$$

Now the value of shear force $V_r$ can be obtained from the equilibrium equation of vertical forces as

$$V_r = -\frac{qr}{2} - T_r\,\frac{\mathrm{d}W}{\mathrm{d}r} + \frac{D}{r}\,. \tag{64}$$

The value of $D$ in equation (64) is obtained using equation (55) and the conditions that at $r = \rho$, $V = 0$ and $T_\rho = T_0$. Hence

$$D = -\frac{T_0 W_\rho}{(R/\rho - 1)} + \frac{q\rho^2}{2}\,. \tag{65}$$

Substitution of the value of $D$ in equation (64) yields

$$V_r = -\frac{qr}{2} - T_r\,\frac{dW}{\mathrm{d}r} - \frac{T_0 W_\rho}{(R/\rho - 1)} + \frac{q\rho^2}{2r}\,. \tag{66}$$

Using equation (66) in equation (43), the equilibrium of the cone is written as

$$\frac{\mathrm{d}}{\mathrm{d}r}\,(rM_r) - M_\theta + rT_r\,\frac{\mathrm{d}W}{\mathrm{d}r} + \frac{T_0 W_\rho}{((R/\rho) - 1)} = \frac{q\rho^2}{2} - \frac{qr^2}{2}\,. \tag{67}$$

The value of $M_\theta$ appearing in the above equation is determined by substituting the value of $P_\theta$ in equation (60) into equation (16). The value of $T_r$ is obtained from equation (61). The values of $M_\theta$, $T_r$ so obtained are substituted in equation (67) and integrated. Using the two remaining boundary conditions, namely,

$$(M_r)_{r=R} = 0 \tag{68}$$

and $$(M_r)_{r=\rho} = M_{\min} = M_0(1-\alpha-\beta) \tag{69}$$

the value of $Q_m$ is obtained as

$$\frac{Q_m}{Q_j} = \frac{1 + \dfrac{1-5\rho/R}{1-\rho/R}\,\beta}{(1+2\rho/R)\,(1-\rho/R)^2}\,. \tag{70}$$

Using equation (70) for different values of $\rho/R$ the total load $Q_m$ can be calculated. The corresponding central deflection $\delta = (\delta_j + \delta_p)$ can be found out by using equations (58), (63) and (55). From equation (58),

$$\frac{W_\rho}{R-\rho} = B_2 \frac{4\beta M_0}{T_0^2} . \tag{71}$$

Substituting the value of $B_2$ from equation (68) and simplifying

$$\frac{W_\rho}{R-\rho} = \frac{8\beta M_0}{(1-\rho/R)^2 T_0 R} . \tag{72}$$

The value of $M_0$ appearing in equation (72) may be written in the form

$$M_0 = \frac{A_s f_s \, \mathrm{d}}{\left[\dfrac{\mathrm{d}/\mathrm{d}_1}{1 - \dfrac{3}{4}\dfrac{A_s f_s}{\mathrm{d}_1 f_c}}\right]} = \frac{T_0 \mathrm{d}}{k} . \tag{73}$$

Substituting the value of $M_0$ from equation (73) in equation (72) and simplifying,

$$\frac{W_\rho}{R} = \frac{8(\beta/k)\,(\mathrm{d}/R)}{(1-\rho/R)} . \tag{74}$$

Now the value of $\delta$ is obtained using equation (74) and equation (49) as

$$\frac{\delta}{R} = \frac{\delta_j + \delta_p}{R} = \frac{8(\beta/k)\,(\mathrm{d}/R)}{1-\rho/R} + \frac{q\rho^2}{4RT_0} . \tag{75}$$

Substituting the value of $T_0$ in terms of $M_0$ from equation (73), equation (75) reduces to

$$\frac{\delta}{\mathrm{d}} = \frac{8\beta/k}{1-\rho/R} + \frac{3}{2k}\,\frac{Q_m}{Q}\,\frac{\rho^2}{R^2} . \tag{76}$$

Hence the load-deflection behaviour beyond Johansen's load can be estimated from equations (64) and (76), the procedure for which is as follows: For a given slab, the values $\beta$ and $k$ are computed using the strength and sectional properties of the slab. A value of $\rho/R$ is assumed and the value of $Q_m$ is estimated from equation (70). The corresponding deflection $\delta$ is obtained by substituting the value of $Q_m$ and the assumed value of $\rho/R$ in equation (76). Thus coordinates of one point are obtained in the

load-deflection plot. The above procedure is repeated for different values of $\rho/R$ and the load-deflection behaviour beyond Johansen's load is obtained.

## 3. Experimental work

The experimental programme consisted of casting and testing 14 isotropic and orthotropic circular slabs. These covered two ratios of radius to thickness of slab, namely, 12.58 and 16.09. The coefficients of orthotropy were varied such that the cases covered include $M_1 < M_2$, $M_1 = M_2$ and $M_1 > M_2$. The details of casting and testing of these slabs are reported elsewhere[19] and hence are not repeated. Table I gives the details of the tested slabs. Out of these slabs, four slabs with $M_1 = M_2$ correspond to the case of isotropy the analysis of which is presented in this paper.

## 4. Results

### *4.1. Comparison of load-deflection behaviour*

The proposed method has been used to predict the load-deflection curves for the tested slabs. The comparison is shown in fig. 3 for slab SSl. Also other solutions based on rigid plastic approach namely that of Wood[11] and Braestrup and Morley[16] have also been used to predict the load-deflection behaviour beyond Johansen's load and plotted in fig. 3 for

**Table I**
**Details of simply supported circular slabs of Series 1**

| Slab no. | Thickness (mm) | Spacing of reinforcement (mm) | | Percentage of reinforcement | | Cube strength ($N/mm^2$) | Intensity of computed Johansen's load ($KN/m^2$) | $Q_{uc}$ (KN) | $\delta_{uc}$ (mm) |
|---|---|---|---|---|---|---|---|---|---|
| | | along circumferential direction | along radial direction | Circumferential | Radial | | | | |
| SS1 | 65.0 | 101.6 | 101.6 | 0.248 | 0.230 | 22.4 | 38.5 | 112.0 | 55.0 |
| SS2 | 65.0 | 101.6 | 50.8 | 0.248 | 0.457 | 25.0 | 38.7 | 106.0 | 42.5 |
| SS3 | 65.0 | 101.6 | 76.2 | 0.248 | 0.306 | 21.5 | 38.4 | 101.5 | 48.0 |
| SS4 | 65.0 | 50.8 | 101.6 | 0.494 | 0.230 | 28.7 | 58.8 | 176.0 | 50.0 |
| SS5 | 65.0 | 50.8 | 50.8 | 0.494 | 0.457 | 26.2 | 74.1 | 186.0 | 55.0 |
| SS6 | 65.0 | 38.1 | 101.6 | 0.660 | 0.230 | 21.8 | 73.5 | 188.0 | 31.0 |
| SS7 | 65.0 | 76.2 | 101.6 | 0.330 | 0.230 | 21.8 | 48.2 | 127.0 | 46.0 |
| SS8 | 50.8 | 101.6 | 76.2 | 0.346 | 0.415 | 33.9 | 25.5 | 131.0 | 46.0 |
| SS9 | 50.8 | 101.6 | 101.6 | 0.346 | 0.312 | 30.9 | 25.4 | 111.0 | 46.0 |
| SS10 | 50.8 | 76.2 | 101.6 | 0.461 | 0.312 | 32.0 | 30.1 | 130.0 | 50.0 |
| SS11 | 50.8 | 38.1 | 101.6 | 0.922 | 0.312 | 20.7 | 40.0 | 176.0 | 53.0 |
| SS12 | 50.8 | 50.8 | 101.6 | 0.690 | 0.312 | 27.1 | 37.5 | 164.0 | 70.0 |
| SS13 | 50.8 | 50.8 | 50.8 | 0.690 | 0.621 | 25.5 | 43.4 | 172.0 | 71.0 |
| SS14 | 50.8 | 101.6 | 50.8 | 0.346 | 0.621 | 25.9 | 23.6 | 129.0 | 50.0 |

Note: Average cover up to centre of radial reinforcement is 11 mm, radius of slab = 820 mm, $\phi$ of reinforcement = 4 mm.

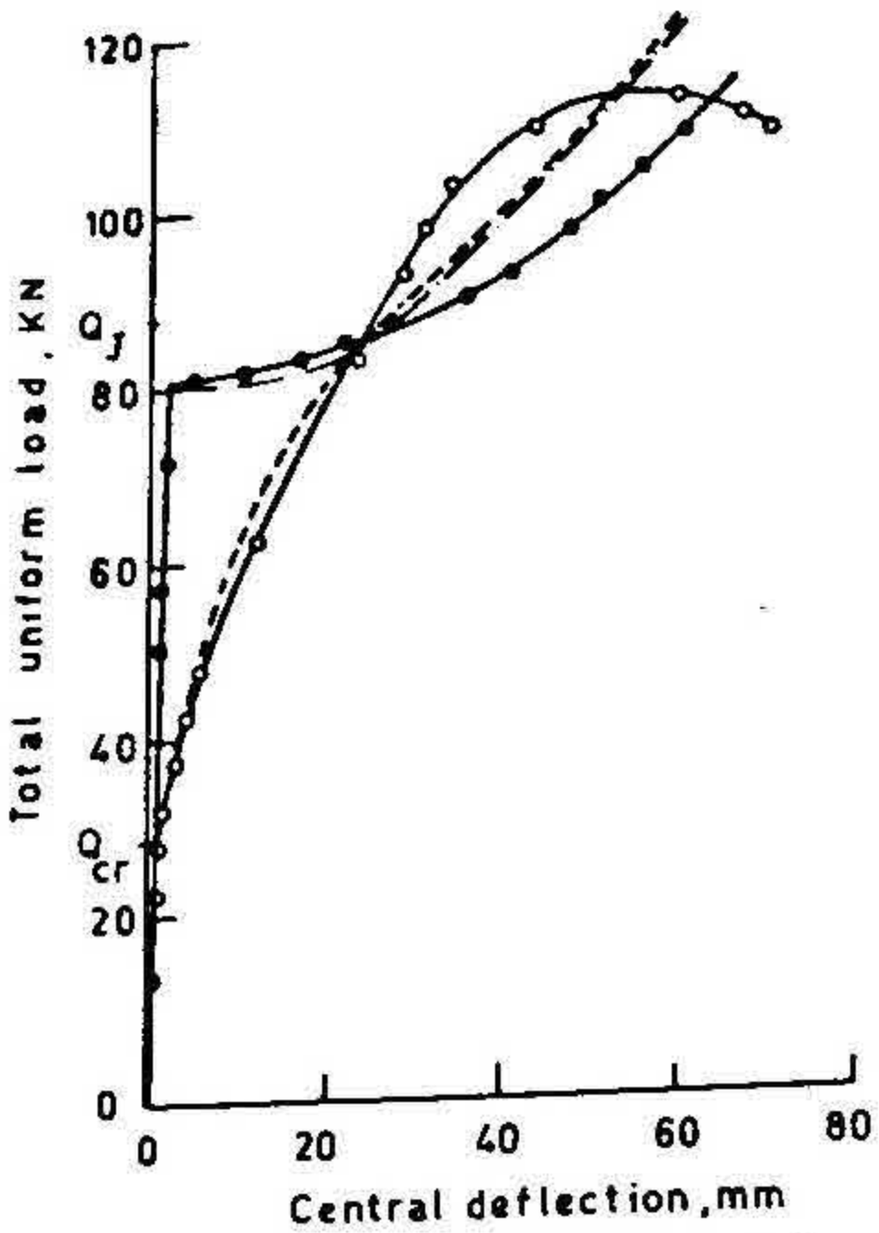


FIG. 3. Comparison of experimental and computed load-deflection curves for slab SS-1. —o— Experimental; ----- Proposed; —•— Braestrup and Morley; —·— Wood.

comparison. It is noted that the proposed method predicts the load-deflection behaviour more satisfactorily than other methods for most of the tested slabs. As the theoretical curves do not show the descending trend of the curve, the curves have been terminated at the experimental deflections at failure load.

### *4.2. Determination of ultimate load*

The ultimate loads of simply supported circular slab have been computed. For this purpose the deflection at ultimate has been taken as 0.9 d as determined in Table II which is the average value of deflection at ultimate load for all the 14 slabs tested in this study. The ratios of experimental ultimate load $Q_{ue}$ to the predicted ultimate load $Q_{up}$ have been determined and are given in Table III. Other methods available in the literature have also been used to estimate ultimate load, namely, those of Wood[11] and Braestrup and Morley[16]. It is found from Table III, that all the three methods underestimate the ultimate load slightly and hence may be considered satisfactory.

### *4.3. Certain limitations of the proposed analysis*

It may be seen from fig. 3 that the proposed analysis, as well as the other methods available in literature, give a load-deflection plot which is concave beyond yield-line load, whereas, the experimental plot is convex. Hence, the presently available procedures based on 'perfectly plastic behaviour' do not result in a load-deflection plot

**Table II**
**Ratio of deflection to thickness of slabs at ultimate**

| Slab no | Deflection mm ($\delta_{uc}$) | Thickness mm ($d$) | Ratio $\delta_{uc}$/d |
|---|---|---|---|
| SS1 | 55.0 | 65.0 | 0.85 |
| SS2 | 42.5 | 65.0 | 0.65 |
| SS3 | 48.0 | 65.0 | 0.74 |
| SS4 | 50.0 | 65.0 | 0.77 |
| SS5 | 55.0 | 65.0 | 0.85 |
| SS6 | 31.0 | 65.0 | 0.48 |
| SS7 | 46.0 | 65.0 | 0.71 |
| SS8 | 46.0 | 50.8 | 0.91 |
| SS9 | 46.0 | 50.8 | 0.91 |
| SS10 | 50.0 | 50.8 | 0.99 |
| SS11 | 53.0 | 50.8 | 1.04 |
| SS12 | 70.0 | 50.8 | 1.38 |
| SS13 | 71.0 | 50.8 | 1.40 |
| SS14 | 50.0 | 50.8 | 0.99 |
| Average | | | 0.90 |

which would clearly show a maximum load and the descending part of the curve beyond the maximum. This has necessitated the introduction of a deflection at maximum load—a data which is based on the average of test results. These data require to be defined more completely with respect to strength of concrete, amount of reinforcement, radius/thickness ratio of the slab and other parameters which affect the load-deflection behaviour of the slab and this can be done only on the basis of large number of test results.

**Table III**
**Ratio of experimental to computed ultimate loads of simply supported isotropic slabs (using $\delta_u = 0.9$ d)**

| Slab number | Ratio of experimental to computed ultimate load | | | |
|---|---|---|---|---|
| | Ultimate load $Q_{ue}$ (KN) | Proposed method $Q_{ue}/Q_{up}$ | Wood's method $Q_{ue}/Q_{uw}$ | Braestrup and Morley's method $Q_{ue}/Q_{ubm}$ |
| SS1 | 112.0 | 0.97 | 0.97 | 1.07 |
| SS5 | 186.0 | 0.98 | 0.98 | 0.96 |
| SS9 | 111.0 | 1.43 | 1.43 | 1.63 |
| SS13 | 172.0 | 1.67 | 1.67 | 1.67 |
| Average | | 1.26 | 1.26 | 1.33 |

Future investigations on this problem could attempt methods in which the perfectly plastic behaviour assumption is probably abandoned or modified and alternate procedures developed which would result in load-deflection plots that represent the experimental plots much better than what could be obtained in the present investigation.

## 5. Conclusions

1. The proposed membrane analysis is an extension of Wood[11] and takes into consideration the deflections occurring up to yield-line load. The load-deflection plots up to ultimate load obtained by the proposed method give satisfactory agreement with the test results. This agreement is better than that given by two other methods available in literature.

2. The deflection at ultimate load has been obtained as a proportion of slab thickness. The average value of deflection at ultimate is 0.9 d for the slab tests conducted in this investigation.

3. The proposed method has been used to predict the ultimate loads of simply supported isotropic circular slabs using $\delta_u$/d as 0.9. It is noted that the proposed method underestimates the ultimate load by 26%. Two other methods available in literature *viz.*, those due to Wood and Braestrup and Morley underestimate by 26 and 33%, respectively. Thus, all the three methods may be considered satisfactory as the error in estimation of ultimate load is on the safe side only.

4. It is noticed that the proposed method and other methods available in literature, which are based on perfectly plastic behaviour assumption have resulted in a load-deflection plot which is concave (and not convex) beyond the yield-line load. Future investigations on this problem could attempt at developing alternate analytical procedures which would result in load-deflection plots that represent better the experimental plots.

### Notation

| | | |
|---|---|---|
| $A, a, B$ | : | Coefficients |
| $A_1, A_2, a_1, B_1, B_2$ | : | Constants |
| $A_s$ | : | Area of steel |
| $C, C_1$ | : | Arbitrary constants |
| d | : | Thickness of slab |
| $d_1$ | : | Effective depth |
| $E_c$ | : | Modulus of elasticity of concrete |
| $f$ | : | Yield function . |
| $f_c$ | : | Cube strength |
| $f'_c$ | : | Cylinder strength |
| $f_r$ | : | Modulus of rupture |
| $f_y$ | : | Yield stress |
| $I_{cr}, I_{eff}, I_g$ | : | Cracked moment of inertia, effective moment of inertia, gross moment of inertia, respectively |

$K_\theta$ : Curvature in circumferential direction
$K_s$ : Constant depending on the properties of the section
$M$ : Plastic moment capacity of the section about the centre line
$M_r$ : Radial moment
$M_0$ : Moment capacity of the section with zero membrane forces
$M_\theta$ : Moment in circumferential direction
$M_1, M_2$ : Moment capacity of the section in circumferential and radial directions, respectively
$m_\theta, m_r$ : Circumferential and radial elastic moment, respectively
$P$ : Compressive force
$P_\theta$ Compressive force in circumferential direction
$Q, Q_j, Q_m, Q_{ue}$ : Applied load, Johansen's load (yield-line load), membrane load, experimental ultimate load, respectively
$q, q_{cr}, q_j$ : Intensity of load, cracking load and Johansen's load, respectively
$R$ Radius of circular slab
$r$ Radius
$T_0$ : Uniaxial tension
$T_r, T_\theta$ : Tensile force in radial and circumferential directions, respectively
$t$ : steel index
$u, u_0$ : Radial displacement, displacement at centre, respectively
$V_r$ Shear force per unit length
$W$ : Deflection of mechanism
$Y_t$ : Distance to the neutral axis from the extreme fibre
$\alpha, \beta, \beta_1, \gamma$ Coefficients
$\delta, \delta_{cr}, \delta_j, \delta_p, \delta_u, \delta_{ue}, \varepsilon_r, \varepsilon_\theta$ : Deflection, deflection at cracking load, deflection at Johansen's load, plastic deflection, deflection at ultimate load, experimental deflection at ultimate load, strains in radial, and circumferential directions, respectively
$\rho$ : Radius of cone
$\mu$ Poisson's ratio
$\mu_0$ : Depth of neutral axis above mid-depth at the centre of slab
$\mu_\theta$ : Height of neutral axis above mid-depth along circumferential direction

## References


1. JOHANSEN, K. W. *Yield-line theory*, Cement and Concrete Association, London, 1962.
2. DESAYI, P. AND KULKARNI, A. B. Membrane action, deflections and cracking of two-way reinforced concrete slabs, *Mater. Struct.*, (RILEM, Paris), 1977, **59**, 303–312.
3. PARK, R. Ultimate strength of rectangular concrete slabs under short-term loading with edges restrained against lateral movement, *Proc. Instn Civ. Engr* (*Lond.*), 1964, **28**, 125–150.
4. TAYLOR, R., MAHER, D. R. H. AND HAYES, B. Effect of arrangement of reinforcement on the behaviour of reinforced concrete slabs, *Mag. Concr. Res.*, 1966, **18**, 85–94.
5. HAYES, B. Allowing for membrane action in the plastic analysis of rectangular reinforced concrete slabs, *Mag. Concr. Res.*, 1968, **20**, 205–211.
6. KEMP, K. O. Yield of square reinforced concrete slab on simple supports allowing for membrane action, *Struct. Engr*, 1967, **145**, 235–240.
7. SAWCZUCK, A. AND WINNICKI, L. Plastic behaviour of simply supported plates at moderately large deflexions, *Int. J. Solids Struct.*, 1965, **1**, 97–111.
8. MORLEY, C. T. Yield line theory for reinforced concrete slabs at moderately large deflexions, *Mag. Concr. Res.*, 1967, **19**, 211–222.
9. DESAYI, P. AND KULKARNI, A. B. Load-deflection behaviour of simply supported rectangular reinforced concrete slabs, *Proc. Int. Ass. Bridge Struct. Engng—1*, 1978, p. 11/78, 1–16.
10. PRABHAKARA, A. *Strength and deformation of reinforced concrete skew slabs*, Ph.D. Thesis, Indian Institute of Science, Bangalore, 1979, pp. 154–160.
11. WOOD, R. H. *Plastic and elastic design of slabs and plates*, Thames and Hudson, London, 1961.
12. DESAYI, P. AND KULKARNI, A. B. Effect of membrane action on plastic collapse load of circular orthotropic slabs with fixed edges, *Int. J. Mech. Sci.*, 1978, **20**, 97–108.
13. JANAS, M. Large plastic deformations of reinforced concrete slabs, *Int. J. Solids Struct.*, 1968, **4**, 61–74.
14. CALLADINE, C. R. Simple ideas in the large-deflection plastic theory of plates and slabs, in *Engineering plasticity*, Heyman and Leckie (eds), Cambridge University Press, Cambridge, England, 1968, pp. 93–127.
15. AL-HASSANI, H. M. *Behaviour of axially restrained slabs*, Ph.D. Thesis, University of London, 1978.
16. BRAESTRUP, M. W. AND MORLEY, C. T. Dome effect in RC slabs; elastic-plastic analysis, *J. Struct. Div.*, ASCE, 1980, **106** (ST6), 1255–1262.
17. CHATTOPADHYAY, B. Discussion on ref. 11, *J. Struct. Div.*, ASCE, 1981, **107** (ST5), 1019.
18. TIMOSHENKO, S. AND WOINOWSKY-KREIGER, S. *Theory of plates and shells*, International Student Edition, Second Edition, McGraw-Hill Kogakusha Ltd, 1959.
19. DESAYI, P. AND MUTHU, K. U. Short-time deflections of reinforced concrete slabs, *Proc. Instn Civ. Engr* (Lond.), Part 2, 1981, **71**, 323–340.
20. *Building code requirements of reinforced concrete*, ACI Standard, ACI-318, 1977.